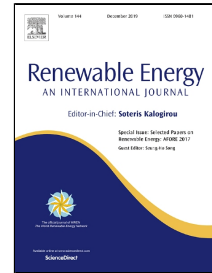


# Journal Pre-proof

A new diffuse luminous efficacy model for daylight availability in Burgos, Spain

M.I. Dieste-Velasco, M. Du00edez-Mediavilla, C. Alonso-Tristu00e1n, D. Gonzu00e1lez-Peu00f1a, M.C. Rodru00edguez-Amigo, T. Garcu00eda-Calderu00f3n



PII: S0960-1481(19)31238-8  
DOI: <https://doi.org/10.1016/j.renene.2019.08.051>  
Reference: RENE 12130

To appear in: *Renewable Energy*

Received Date: 17 May 2019  
Accepted Date: 08 August 2019

Please cite this article as: M.I. Dieste-Velasco, M. Du00edez-Mediavilla, C. Alonso-Tristu00e1n, D. Gonzu00e1lez-Peu00f1a, M.C. Rodru00edguez-Amigo, T. Garcu00eda-Calderu00f3n, A new diffuse luminous efficacy model for daylight availability in Burgos, Spain, *Renewable Energy* (2019), <https://doi.org/10.1016/j.renene.2019.08.051>

This is a PDF file of an article that has undergone enhancements after acceptance, such as the addition of a cover page and metadata, and formatting for readability, but it is not yet the definitive version of record. This version will undergo additional copyediting, typesetting and review before it is published in its final form, but we are providing this version to give early visibility of the article. Please note that, during the production process, errors may be discovered which could affect the content, and all legal disclaimers that apply to the journal pertain.

© 2019 Published by Elsevier.

1 **A new diffuse luminous efficacy model for daylight availability in Burgos,**  
2 **Spain**

3  
4 M.I. Dieste-Velasco<sup>a\*</sup>; M. Díez-Mediavilla<sup>a</sup>; C. Alonso-Tristán<sup>a</sup>; D. González-Peña<sup>a</sup>,  
5 M.C. Rodríguez-Amigo<sup>a</sup>, T. García-Calderón<sup>a</sup>

6 <sup>a</sup>Solar and Wind Feasibility Technologies Research Group (SWIFT). Electromechanical Engineering  
7 Department. University of Burgos, Avda. de Cantabria s/n Burgos, Spain.

8  
9 \*Corresponding author: [midieste@ubu.es](mailto:midieste@ubu.es)

10  
11 **Abstract**

12 The determination of optimal illumination conditions in buildings is of great interest both  
13 for reducing energy consumption and for exploiting solar resources with greater  
14 efficiency and sustainability. The most commonplace method of estimating daylight is  
15 the luminous efficacy approach, using the more widely measured solar irradiance. In this  
16 present study, a new model of diffuse luminous efficacy over a horizontal surface is  
17 proposed. A comparative study of twenty-two classic models is presented, to obtain  
18 diffuse illuminance, using both, the original mathematical models and the adapted  
19 models with local coefficients, in order to determine the most suitable models for Burgos,  
20 a city located in north-western Spain. With this purpose in mind, twelve models are  
21 selected for all sky conditions, five models for modelling clear sky, two for partly cloudy  
22 sky, and three for overcast sky. These twenty-two models are then compared with the  
23 new model both for all sky conditions and for particular sky conditions (clear, partly  
24 cloudy, and overcast). The behaviour of the new model showed greater accuracy than  
25 most of the classic models under analysis. Hence, the advantage of the diffuse luminous  
26 efficacy model that can be applied both to all sky and to particular sky conditions.

27  
28  
29 **Keywords:** Luminous Efficacy Models, Diffuse Illuminance, Irradiance, Modelling  
30

31

**Nomenclature** $a_i, b_i, c_i, d_i$ : Perez's coefficients $D$ : cloud ratio or sky ratio or diffuse fraction $E_{bh}$ : horizontal beam irradiance ( $W/m^2$ ) $E_{dh}$ : horizontal diffuse irradiance ( $W/m^2$ ) $E_{gh}$ : horizontal global irradiance ( $W/m^2$ ) $I$ : normal incidence direct irradiance ( $W/m^2$ ) $I_0$ : extraterrestrial irradiance ( $W/m^2$ ) $K_d$ : diffuse luminous efficacy ( $lm/W$ ) $K_D$ : ratio of diffuse to extraterrestrial irradiance $K_t$ : clearness index $L_{bh}$ : horizontal beam illuminance ( $lux$ ) $L_{dh}$ : horizontal diffuse illuminance ( $lux$ ) $L_{gh}$ : horizontal global illuminance ( $lux$ ) $m$ : relative optical airmass $MBE$ : Mean Bias Error (%) $n$ : number of data $p_0, p_1, p_2, p_3$ : coefficients of the new model $RMSE$ : Root Mean Square Error (%) $T_d$ : three-hourly surface dew point temperature ( $^{\circ}C$ ) $W$ : atmospheric precipitable water ( $cm$ ) $X_{measured}$ : measured variable $X_{model}$ : predicted variable $Z$ : solar zenith angle ( $rad$ ) $\alpha$ : solar altitude angle ( $rad$ ) $\Delta$ : sky brightness $\varepsilon$ : sky clearness $\Omega$ : relative heaviness of overcast sky

32

**1. Introduction**

34 Maximization of natural lighting coupled with sustainable and ecological development for  
 35 the reduction of energy consumption are now essential building design strategies [1].  
 36 Bearing these aims in mind, artificial light should be used to complement daylight, in  
 37 order to maintain rather than increase energy demand [2]. When considering the design  
 38 of energy efficient buildings, which rely on daylight, and efficient sizing of both cooling  
 39 and heating systems, quantitative information is necessary on the levels of illumination  
 40 and solar irradiance received on surfaces with different inclinations. Horizontal  
 41 illuminance data, among many other uses, are of particular importance for the study and  
 42 the development of solar roofs and skylights. Illuminance data processed by specialized  
 43 software for interior lighting calculations [3], will provide more sustainable, healthy, and  
 44 energy efficient buildings; natural lighting in buildings will therefore contribute to  
 45 energetic and environmental objectives. However, illuminance is not an easily measured  
 46 parameter, since the number of facilities devoted to illuminance measurements is scarce  
 47 compared to those available for radiance measurements. An alternative method to  
 48 increase illuminance data is through the use of luminous efficacy. Once the ratio of  
 49 luminance to irradiance (i.e. luminous efficacy ( $K_d$ )), is known, then the measured  
 50 irradiance ( $E_{dh}$ ) values can be converted to illuminance values ( $L_{dh}$ ) as defined by  
 51 Equation (1).

52

$$K_d = \frac{L_{dh}}{E_{dh}} \quad (\text{lm/W}) \quad (1)$$

53

54 Over the past few years, there has therefore been a tendency to develop luminous  
55 efficacy models that are based on experimental irradiance measurements, from which  
56 the illuminance data can then be obtained.

57 In this present study, twenty-two classic models from the literature are reviewed and  
58 tested for the city of Burgos (Spain) using both the original form, proposed by the authors  
59 of these models, and their local adaptation to the place under study. Traditional statistical  
60 indicators RMSE (%) and MBE (%) were used to classify the models and to determine  
61 their accuracy. Data measurements over one year and nine months were used in this  
62 study (one year to obtain the local coefficients of the models and nine months for their  
63 validation). In addition, a new model to predict diffuse horizontal illuminance to the sky  
64 conditions of the city of Burgos is proposed in this present study. This new model is  
65 analysed for all sky conditions and for particular sky conditions (clear, partly cloudy, and  
66 overcast), showing improved illuminance prediction over most of the twenty-two  
67 previously tested models.

68 The study will be structured as follows: First a literature review of classic models will be  
69 conducted in Section 2. Then, in Section 3, the experimental meteorological facility and  
70 the data used for the study will be described. In Section 4, the diffuse luminous efficacy  
71 models on horizontal surfaces that are reviewed in this work will be presented. The  
72 results of benchmarking the twenty-two luminous efficacy models under review will then  
73 be discussed in Section 5. The new model will be proposed in Section 6 for the area  
74 under study and compared with the other models under review. In Section 7, validation  
75 of both the new model and the twenty-two luminous efficacy models will be presented  
76 and, finally, the main conclusions of this study will be outlined.

77

## 78 **2. Literature review**

79 Various studies on the analysis of diffuse luminous efficacy have been developed,  
80 among which those of Pérez et al. [4] should be mentioned. Those authors proposed  
81 different models to analyse global, diffuse, and beam luminous efficacy for all sky  
82 conditions, as a function of the atmospheric precipitable water content, the sky  
83 brightness, and the zenith angle. Their models were developed from experimental  
84 measurements in geographical locations around the USA and Europe with different  
85 weather conditions [4]. Chung proposed another interesting model [5] to measure

86 luminous efficacy in Hong Kong. The model he developed is applicable to different sky  
87 types, which are classified according to the cloud ratio or sky ratio, defined as the ratio  
88 between horizontal diffuse irradiance and horizontal global irradiance [5]. Lam and Li  
89 also developed luminous efficiency models with constant values for the city of Hong  
90 Kong [6]. The sky classification that these authors employed was based on the clearness  
91 index ( $K_t$ ), defined as the ratio between global and extraterrestrial irradiance [7].  
92 Likewise, the research of Muneer and Kinghorn [8] proposed a diffuse luminous efficacy  
93 model for five UK stations where the clearness index was shown to be the main  
94 parameter influencing both global and diffuse luminous efficacy.

95 Further studies, such as those of Robledo and Soler [9] developed luminous efficacy  
96 models from irradiance and illuminance measurements for Madrid (Spain). These  
97 authors employed two independent variables, solar altitude and sky brightness. Their  
98 models produced better predictions for clear skies than other models, developed by the  
99 same authors, which only employed solar altitude as independent variable. However,  
100 they recommended the simplified model for partly cloudy sky and overcast sky, which  
101 only takes account of sky brightness [9]. In contrast, the work of Ruiz et al. [10] showed  
102 the suitability of both the Muneer and the Kinghorn models [8] to determine the diffuse  
103 luminous efficacy in Madrid (Spain). Moreover, Ruiz et al. also developed and evaluated  
104 other models based on that of Muneer and Kinghorn [8]. In addition, the same authors  
105 showed that using the ratio between diffuse and extraterrestrial irradiance ( $K_D$ ) improved  
106 the diffuse luminous efficacy prediction, compared with the results generated with the  
107 clearness index [10].

108 In turn, Souza and Robledo [11] evaluated the luminous efficacy models proposed by  
109 Muneer and Kinghorn [8], Chung [5], Ruiz et al. [10], and Robledo and Soler [9] in the  
110 city of Florianapolis (Brazil). They showed that when using local optimized coefficients  
111 for Florianapolis, the model of Robledo and Soler [9] provided better statistical results  
112 and was at the same time the model that best predicted the behaviour of the luminous  
113 efficacy values for all solar altitudes. In another work, Souza and Robledo [11] evaluated  
114 several models specifically obtained for clear skies and showed that the results of these  
115 models were no better than those obtained with all sky models when used to estimate  
116 illuminance for clear sky [11]. Other authors used a constant value to model the diffuse  
117 luminous efficacy: De Rosa et al. [12] proposed a constant value for all sky, clear sky,  
118 intermediate, and overcast sky conditions in Arcavacata di Rende (Italy) and compared  
119 those values with others from Geneva (Switzerland), Vaulx-en-Velin (France), Bratislava  
120 (Slovakia), and Osaka (Japan). Likewise, Cucumo et al. [13] employed a constant value  
121 of 127.41 lm/W to predict the diffuse luminous efficacy for all sky conditions in  
122 Arcavacata di Rende (Italy). These authors compared their approach with the results of

123 other models in the literature and concluded that the use of a constant value to estimate  
124 diffuse luminous efficacy is valid as an initial estimation of diffuse illuminance [13]. Fakra  
125 et al. [14] offers a further example, estimating an average diffuse luminous efficacy value  
126 of 139.98 lm/W for Saint-Pierre (Reunion Island). The study likewise examined different  
127 indices to classify the sky types. Among their results, the authors pointed out that the  
128 diffuse fraction was the most appropriate index to define the sky types for that  
129 geographical location [14]. Those authors also observed that the luminous efficacy  
130 values remained constant during the day, but varied significantly at sunrise and sunset,  
131 as a function of solar altitude. This fact may be used to explain the deviations that exist  
132 when a constant value is employed to model luminous efficacy [14]. Another constant  
133 value for modelling diffuse luminous efficacy was proposed by Azad et al. [15], who  
134 suggested a value of 121.8 lm/W for New Delhi (India).  
135 Mayhoub and Carter [16] analysed the luminous efficacy values at ten geographical  
136 locations in both Europe and North Africa. They proposed three luminous efficacy  
137 models. The first model was based on the solar altitude, the second one employed both  
138 the solar altitude and the cloud amount, and the third model employed the sky clearness  
139 index. They likewise affirmed that the statistical performance of the first model was better  
140 than the other two and had the additional characteristic of simplicity [16].  
141 Further studies such as those of Kong and Kim [17] determined the diffuse luminous  
142 efficacy at Yongin (South Korea) by using the solar altitude, the relative optical air mass,  
143 the sky brightness, and the clearness index as their independent variables. They also  
144 compared their proposed model with other luminous efficacy models in the bibliography,  
145 mentioning that better statistical results were provided by the model of Muneer and  
146 Kinghorn [8] at this geographical location [17]. In turn, in a study by Patil et al. [18], the  
147 luminous efficacy models of Perez et al. [4], Muneer and Kinghorn [8], and Littlefair [19]  
148 were analysed. The models were locally evaluated with experimental data from six  
149 stations, covering different climatic conditions in India. Those authors mentioned in their  
150 results that the model of Perez et al. was the best from among the three models  
151 discussed in their study [18]. Finally, in the study of Chaiwiwatworakul and  
152 Chirarattananon [20] a diffuse luminous efficacy model was proposed for Bangkok  
153 (Thailand) for all sky conditions, as a function of the sky clearness and the zenith angle  
154 values.

155

### 156 **3. Daylight diffuse illuminance and solar diffuse irradiance measurements**

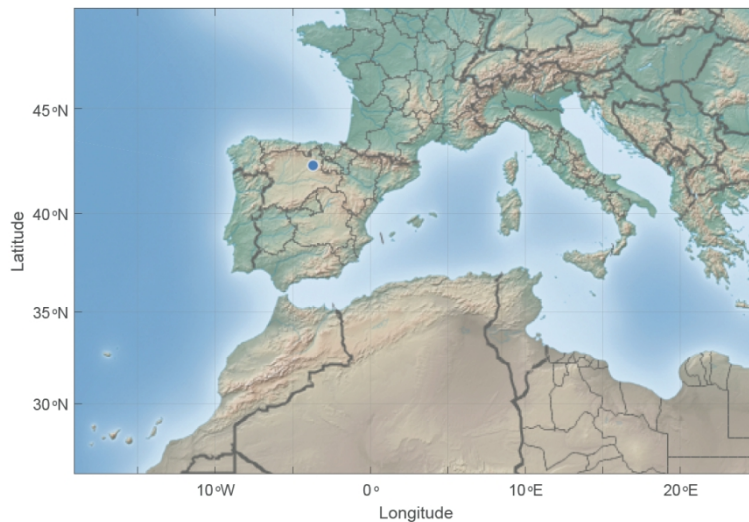
157 A meteorological and radiometric facility, shown in Figure 1, was used to collect the  
158 experimental data used in this present study. This equipment was placed on the roof of  
159 the Higher Polytechnic School building at Burgos University (Spain), (latitude and

160 longitude:  $42^{\circ}21'04''\text{N}$  and  $3^{\circ}41'20''\text{W}$ ), located at 856 m above mean sea level as shown  
 161 in Figure 2.

162



163  
 164 Figure 1. Experimental Equipment  
 165



166  
 167 Figure 2. Burgos (Spain) ( $42^{\circ}21'04''\text{N}$ ;  $3^{\circ}41'20''\text{W}$ ; 856 m above mean sea level)  
 168

169 Temperature, wind velocity and direction, atmospheric pressure, humidity and rainfall  
 170 were measured. Moreover, global, beam, and diffuse horizontal irradiance ( $E_{gh}$ ,  $E_{bh}$ ,  $E_{dh}$ )  
 171 , and illuminance data ( $L_{gh}$ ,  $L_{bh}$ ,  $L_{dh}$ ) were all recorded [21]. Class 1 Hukseflux SR11  
 172 pyranometers and an EKO ML020SO Luxmeter were employed to measure irradiance  
 173 and illuminance data. The facility includes a SONA201D All Sky Camera Day and a MS-  
 174 321LR sky scanner, both from EKO. The experimental data were recorded on a  
 175 CAMPBELL CR3000 datalogger. These experimental data were measured, from 1<sup>st</sup> April

176 2017 to 31<sup>st</sup> March 2018, with a sampling time of thirty seconds. Average values were  
 177 recorded every 10 minutes, for determination of the diffuse luminous efficacy models.  
 178 The same experimental procedure was followed between 1<sup>st</sup> April 2018 and 31<sup>st</sup>  
 179 December 2018, in order to measure the data for testing the models. The experimental  
 180 values of  $E_{gh}$ ,  $E_{bh}$ ,  $E_{dh}$ , and  $L_{gh}$ ,  $L_{bh}$ ,  $L_{dh}$  were analysed and filtered using traditional quality  
 181 criteria [22].

182

#### 183 **4. Diffuse luminous efficacy models on horizontal surfaces**

184 The twenty-two classic luminous efficacy models analysed in this present study  
 185 encompass models that use solar altitude as their only independent variable, models  
 186 that employ other parameters such as sky brightness, sky clearness, diffuse fraction,  
 187 zenith angle and clearness index, and models that propose a constant value for  
 188 modelling luminous efficacy. Moreover, the models analysed in this study are applied  
 189 either to particular sky conditions (clear sky, partly cloudy sky, and overcast sky) or to all  
 190 sky conditions.

191

192 The models under review are presented in two ways: either by using the original  
 193 coefficients given by their authors or adapted to local conditions. The previously  
 194 described experimental data were used to calculate the local coefficients of the model.  
 195 The data were fitted with non-linear least squares method using the Matlab™ R2018b fit  
 196 function.

197

##### 198 **4.1. Perez et al. model (1990)**

199 Perez et al. [4] modelled diffuse luminous efficacy with Equation (2), where  $a_i$ ,  $b_i$ ,  $c_i$ ,  $d_i$   
 200 are the original coefficients of the model shown in Table 1(a). The local adaptation of  
 201 these coefficients to the city of Burgos, is presented in Table 1(b). In this model,  $W$  is the  
 202 atmospheric precipitable water content, which may be obtained from Equation (3),  $Z$  is  
 203 the solar zenith angle, and  $\Delta$  is the sky brightness, which can be obtained from  
 204 Equation (4).

205

$$K_d = a_i + b_i W + c_i \cos(Z) + d_i \ln(\Delta) \quad (lm/W) \quad (2)$$

206

$$W = e^{(0.07T_d - 0.075)} \quad (3)$$

$$\Delta = \frac{E_{dh} * m}{I_0} \quad (4)$$

207 Perez et al. classified the different sky types by using the sky clearness parameter, which  
 208 is shown in Equation (5), where  $k = 1.041$  for  $Z$  in radians [4].  
 209

$$\varepsilon = [(E_{dh} + I)/E_{dh} + kZ^3]/[1 + kZ^3] \quad (5)$$

210

Table 1. Perez et al. model (1990)

$\varepsilon$ category	Lower bound	Upper bound	a) Original diffuse luminous efficacy coefficients				b) Local diffuse luminous efficacy coefficients for Burgos, Spain			
			$a_i$	$b_i$	$c_i$	$d_i$	$a_i$	$b_i$	$c_i$	$d_i$
1	1.000	1.065	97.24	-0.46	12.00	-8.91	100.65	1.66	0.41	-8.75
2	1.065	1.230	107.22	1.15	0.59	-3.95	100.29	3.23	-12.62	-14.39
3	1.230	1.500	104.97	2.96	-5.53	-8.77	89.80	4.50	-20.54	-26.82
4	1.500	1.950	102.39	5.59	-13.95	-13.90	94.27	3.67	-28.53	-28.39
5	1.950	2.800	100.71	5.94	-22.75	-23.74	111.36	3.10	-37.40	-20.99
6	2.800	4.500	106.42	3.83	-36.15	-28.83	86.01	4.16	-25.01	-27.07
7	4.500	6.200	141.88	1.90	-53.24	-14.03	138.24	3.02	-35.73	-7.28
8	6.200	---	152.23	0.35	-45.27	-7.98	143.04	2.94	-28.65	-2.97

211

#### 212 4.2. The Chung model (1992)

213 This model uses the sky ratio or diffuse fraction ( $D$ ) to classify the sky types. The diffuse  
 214 fraction is defined as the ratio of horizontal diffuse irradiance over horizontal global  
 215 irradiance, as shown in Equation (6). This author classifies the sky conditions as clear  
 216 ( $D < 0.3$ ), partly cloudy ( $0.3 < D < 0.8$ ), and overcast ( $D > 0.8$ ) [5]. Table 2 shows the  
 217 models and their corresponding adaptation to the city of Burgos.

218

$$D = \frac{E_{dh}}{E_{gh}} \quad (6)$$

219

220 Table 2. Chung model equations for modelling diffuse luminous efficacy,  $K_d$  ( $lm/W$ ), and for the different  
 221 sky conditions. The original coefficients were calculated from the experimental data recorded at Hong Kong.  
 222 The locally adapted coefficients were calculated from the experimental data recorded at Burgos, Spain.

Clear sky	Original model	$K_d = 137$
	Locally adapted model	$K_d = 126.609$
Overcast sky	Original model	$K_d = (102.2 + 0.67\alpha - 0.0059\alpha^2) * (1.18 - 8.7 * 10^{-4}\Omega + 9.3 * 10^{-7}\Omega^2)$

	<i>Locally adapted model</i>	$K_d = (101.340 + 14.113\alpha - 10.079\alpha^2) * (1.140 - 3.45 * 10^{-4}\Omega + 2.44 * 10^{-7}\Omega^2)$
Partly Cloudy sky	<i>Original model</i>	$K_d = 135.3 - 25.7D$
	<i>Locally adapted model</i>	$K_d = 126.368 - 17.861D$

223

224 In the overcast model, Chung employed solar altitude ( $\alpha$ ) and the relative heaviness of  
 225 overcast sky ( $\Omega$ ), obtained from Equation (7), as independent variables. On the other  
 226 hand, he employed the diffuse fraction or cloud ratio ( $D$ ) for partly cloudy sky [5]:

$$\Omega = E_{gh}/\sin \alpha \quad (7)$$

227

#### 228 4.3. Lam and Li model (1996)

229 These authors proposed the following sky-type classification, based on the clearness  
 230 index ( $K_t$ ) as follows [6]: clear sky ( $K_t > 0.65$ ); partly cloudy sky ( $0.3 < K_t \leq 0.65$ ), and  
 231 overcast sky ( $0 < K_t \leq 0.3$ ), where ( $K_t$ ) is defined as the ratio of global to extraterrestrial  
 232 irradiance [7]. The models and their local adaptation to the city of Burgos are presented  
 233 in Table 3.

234

235 Table 3. Lam and Li equations for modelling diffuse luminous efficacy calculations,  $K_d$  ( $lm/W$ ), and for the  
 236 different sky conditions. The original coefficients were calculated from the experimental data recorded at  
 237 Hong Kong. The locally adapted coefficients were calculated from the experimental data recorded at Burgos,  
 238 Spain.

Clear sky	<i>Original model</i>	$K_d = 130.6$
	<i>Locally adapted model</i>	$K_d = 117.122$
Overcast sky	<i>Original model</i>	$K_d = 116.2$
	<i>Locally adapted model</i>	$K_d = 116.244$

239

#### 240 4.4. Muneer and Kinghorn model (1998)

241 The model of Muneer and Kinghorn [8] and its adaptation to the local conditions of  
 242 Burgos are shown in Table 4.

243

244 Table 4. Muneer and Kinghorn equations for modelling diffuse luminous efficacy calculations,  $K_d$  ( $lm/W$ ).  
 245 The original coefficients were calculated from data recorded at five different UK locations. The locally  
 246 adapted coefficients were calculated from the experimental data recorded at Burgos, Spain.

All sky	Original model	$K_d = 130.2 - 39.828K_t + 49.979K_t^2$
	Locally adapted model	$K_d = 127.869 - 72.341K_t + 92.354K_t^2$

247

#### 248 4.5. Robledo and Soler model (2001)

249 The sky conditions employed by Robledo and Soler were based on the sky clearness ( $\varepsilon$ ). These conditions are defined as follows [9]: overcast sky: ( $\varepsilon < 1.20$ ); partly cloudy sky  
 250 ( $1.20 < \varepsilon < 5.0$ ) and clear sky ( $\varepsilon > 5.0$ ), where ( $\varepsilon$ ) is obtained from Equation (5). The  
 251 original expressions and the local adaptation of the models to the city of Burgos are  
 252 presented in Table 5.  
 253

254

255 Table 5. Robledo and Soler equations for modelling diffuse luminous efficacy,  $K_d$  ( $lm/W$ ). The original  
 256 coefficients were calculated from the experimental data recorded at Madrid, Spain. The locally adapted  
 257 coefficients were calculated from the experimental data recorded at Burgos, Spain.

All sky	Original (model 1)	$K_d = 86.68(\sin\alpha)^{-0.034} \Delta^{-0.266}$
	Locally adapted (model 1)	$K_d = 97.101(\sin\alpha)^{-0.046} \Delta^{-0.115}$
All sky	Original (model 2)	$K_d = 91.07 \Delta^{-0.254}$
	Locally adapted (model 2)	$K_d = 100.908 \Delta^{-0.105}$
Clear sky	Original (model 1)	$K_d = 68.30(\sin\alpha)^{-0.175} \Delta^{-0.343}$
	Locally adapted (model 1)	$K_d = 120.187(\sin\alpha)^{-0.187} \Delta^{-0.022}$
Clear sky	Original (model 2)	$K_d = 160.670(\sin\alpha)^{-0.114}$
	Locally adapted (model 2)	$K_d = 127.986(\sin\alpha)^{-0.182}$
Overcast sky	Original model	$K_d = 109.68(\sin\alpha)^{-0.012} \Delta^{-0.116}$
	Locally adapted model	$K_d = 106.433(\sin\alpha)^{-0.001} \Delta^{-0.056}$
Partly cloudy sky	Original model	$K_d = 82.240(\sin\alpha)^{-0.052} \Delta^{-0.296}$
	Locally adapted model	$K_d = 89.786(\sin\alpha)^{-0.110} \Delta^{-0.163}$

258

259 **4.6. Ruiz et al. model (2001)**

260 Ruiz et al. employed two independent variables, solar altitude ( $\alpha$ ) and the ratio between  
 261 diffuse and extraterrestrial irradiance ( $K_D$ ), in order to obtain two all sky type models [10].

262 The equations of the models and their adaptation to the local conditions of Burgos are  
 263 presented in Table 6.

264

265 Table 6. Ruiz et al. equations for modelling diffuse luminous efficacy,  $K_d$  ( $lm/W$ ). The original coefficients  
 266 were calculated from the experimental data recorded at Madrid, Spain. The locally adapted coefficients were  
 267 calculated from the experimental data recorded at Burgos, Spain.

All sky	<i>Original (model 1)</i>	$K_d = 160.61 - 47.05K_D - 196.94K_D^2$
	<i>Locally adapted (model 1)</i>	$K_d = 144.990 - 149.439K_D + 168.178K_D^2$
All sky	<i>Original (model 2)</i>	$K_d = 86.970(\sin\alpha)^{-0.143}K_D^{-0.218}$
	<i>Locally adapted (model 2)</i>	$K_d = 98.109(\sin\alpha)^{-0.048}K_D^{-0.115}$

268

269 **4.7. Souza and Robledo model (2004)**

270 The sky conditions that Souza and Robledo used to classify sky types were overcast sky  
 271 ( $\varepsilon < 1.20$ ), partly cloudy sky ( $1.20 < \varepsilon < 5.0$ ), and clear sky ( $\varepsilon > 5.0$ ) [11]. Table 7 shows  
 272 the original form of the model and its local adaptation to the city of Burgos.

273

274 Table 7. Souza and Robledo equations for modelling diffuse luminous efficacy,  $K_d$  ( $lm/W$ ). The original  
 275 coefficients were calculated from the experimental data recorded at Florianopolis, Brazil. The locally adapted  
 276 coefficients were calculated from the experimental data recorded at Burgos, Spain.

Clear sky	<i>Original model</i>	$K_d = 259.03\alpha^{-0.177}$
	<i>Locally adapted model</i>	$K_d = 132.250\alpha^{-0.125}$

277

278 **4.8. Cucumo et al. model (2008)**

279 Cucumo et al. used a constant value for modelling diffuse luminous efficacy [13]. Their  
 280 model and its local adaptation to the city of Burgos are shown in Table 8.

281

282 Table 8. Cucumo et al. equations for modelling diffuse luminous efficacy,  $K_d$  ( $lm/W$ ). The original  
 283 coefficients were calculated from the experimental data recorded at Aravaca di Rende, Italy. The locally  
 284 adapted coefficients were calculated from the experimental data recorded at Burgos, Spain

285

All sky	<i>Original model</i>	$K_d = 127.410$
	<i>Locally adapted model</i>	$K_d = 115.202$

286

#### 287 4.9. Mayhoub and Carter model (2011)

288 Mayhoub and Carter diffuse luminous efficacy models [16] and the form of their local  
289 adaptation to the city of Burgos are shown in Table 9.

290

291 Table 9. Mayhoub and Carter equations for modelling diffuse luminous efficacy,  $K_d$  ( $lm/W$ ). The original  
292 coefficients were calculated from the experimental data recorded at ten locations in Europe and North Africa.  
293 The locally adapted coefficients were calculated from the experimental data recorded at Burgos, Spain

All sky	<i>Original (model 1)</i>	$K_d = 122.740 + 0.0164\alpha$
	<i>Locally adapted (model 1)</i>	$K_d = 116.732 - 0.285\alpha$
All sky	<i>Original (model 2)</i>	$K_d = 121.830 + 3.5567K_t - 18.305K_t^2 + 29.492K_t^3$
	<i>Locally adapted (model 2)</i>	$K_d = 115.072 - 4.700K_t - 10.500K_t^2 + 46.371K_t^3$

294

#### 295 4.10. Fakra et al. model (2011)

296 Table 10 shows the model of Fakra et al. [14] and its local adaptation to the city of  
297 Burgos.

298

299 Table 10. Fakra et al. equations for modelling diffuse luminous efficacy,  $K_d$  ( $lm/W$ ). The original coefficients  
300 were calculated from the experimental data recorded at Saint-Pierre, Reunion Island. The locally adapted  
301 coefficients were calculated from the experimental data recorded at Burgos, Spain.

All sky	<i>Original model</i>	$K_d = 139.980$
	<i>Locally adapted model</i>	$K_d = 115.202$

302

#### 303 4.11. Chaiwiwatworakul and Chirarattananon model (2013)

304 These authors proposed a diffuse luminous efficacy model as a function of the sky  
305 clearness and the zenith angle [20]. Table 11 shows the original model and its local  
306 adaptation to the city of Burgos.

307

308 Table 11. Chaiwiwatworakul and Chirarattananon equations for modelling diffuse luminous efficacy,  $K_d$   
309 ( $lm/W$ ). The original coefficients were calculated from the experimental data recorded at Bangkok, Thailand.  
310 The locally adapted coefficients were calculated from the experimental data recorded at Burgos, Spain.

All sky	Original model	$K_d = (107.14 + 12.59\varepsilon^{0.24}) + \left(30.35 - \frac{30.1}{\varepsilon^{1.5}}\right)Z$
	Locally adapted model	$K_d = (102.613 + 0.081\varepsilon^{1.872}) + \left(45.171 - \frac{35.962}{\varepsilon^{1.026}}\right)Z$

311

312 **4.12. Kong and Kim model (2013)**

313 These authors proposed a model for all sky conditions as a function of the solar altitude,  
 314 the relative optical air mass, the sky brightness, and the clearness index [17]. Table 12  
 315 shows this model and its local adaptation to the city of Burgos.

316

317 Table 12. Kong and Kim equations for modelling diffuse luminous efficacy calculations,  $K_d$  ( $lm/W$ ). The  
 318 original coefficients were calculated from the experimental data recorded at Yongin, South Korea. The locally  
 319 adapted coefficients were calculated from the experimental data recorded at Burgos, Spain.

All sky	Original model	$K_d = 164.403 + 0.166\alpha - 5.759m - 20.393\Delta - 46.974K_t$
	Locally adapted model	$K_d = 137.549 - 13.101\alpha + 0.673m - 79.543\Delta + 18.539K_t$

320

321 A summary of the main features of the models reviewed and the parameters used by  
 322 each of them is shown in Table 13.

323

324 Table 13. Summary of the diffuse luminous efficacy models reviewed in this work. Literature reference of the  
 325 original model, year, authors, sky type classification, input parameters used in the models, and the location  
 326 where the model was first developed.

Ref.	Year	Authors	Sky types	Model parameters	Location
[4]	1990	Perez et al.	All	$W, Z, \Delta$	USA and Europe
[5]	1992	Chung	Clear	137 $lm/W$	China
			Overcast	$\alpha, \Omega$	
			Partly	$D$	
[6]	1996	Lam and Li	Clear	130.6 $lm/W$	China
			Overcast	116.2 $lm/W$	
[8]	1998	Muneer and Kinghorn	All	$K_t$	UK
[9]	2001	Robledo and Soler (model 1)	All	$\alpha, \Delta$	Spain
[9]	2001	Robledo and Soler (model 2)	All	$\Delta$	Spain
[9]	2001	Robledo and Soler (model 1)	Clear	$\alpha, \Delta$	Spain
		Robledo and Soler (model 2)	Clear	$\alpha$	
		Robledo and Soler	Overcast	$\alpha, \Delta$	
			Partly	$\alpha, \Delta$	
[10]	2001	Ruiz et al. (model 1)	All	$K_D$	Spain
		Ruiz et al. (model 2)	All	$\alpha, K_D$	Spain

[11]	2004	Souza and Robledo	Clear	$\alpha$	Brazil
[13]	2008	Cucumo et al.	All	127.41 $lm/W$	Italy
[16]	2011	Mayhoub and Carter (model 1)	All	$\alpha$	Europe and North Africa
[16]	2011	Mayhoub and Carter (model 2)	All	$K_t$	Europe and North Africa
[14]	2011	Fakra et al.	All	139.98 $lm/W$	Reunion Island
[20]	2013	Chaiwiwatworakul and Chirarattananon	All	$Z, \varepsilon$	Thailand
[17]	2013	Kong and Kim	All	$\alpha, m, \Delta, K_t$	South Korea

327

### 328 5. Evaluation of the twenty-two classic diffuse luminous efficacy models on a 329 horizontal plane

330 The goodness-of-fit of the models was calculated by means of the statistical indicators  
331 MBE (%) (Mean Bias Error) and RMSE (%) (Root Mean Square Error) [14] [23]. MBE  
332 shows the trend of the model either to over-estimate or to under-estimate the data. In  
333 contrast, RMSE provides a measure of the deviation between the predicted values using  
334 the fitted models and the experimental measurements. Equations (8) and (9) show the  
335 statistical estimators employed in this present study.

$$MBE (\%) = 100 \frac{\sum_n (X_{model} - X_{measured})}{\sum_n X_{measured}} \quad (8)$$

$$RMSE (\%) = 100 \frac{\sqrt{\frac{\sum_n (X_{model} - X_{measured})^2}{n}}}{\frac{\sum_n X_{measured}}{n}} \quad (9)$$

336 Tables 14-17 present the results of applying the statistical estimators shown in  
337 Equations (8) and (9) to the models analysed in this study. Table 14 shows the results  
338 obtained for all sky conditions (twelve models). It can be observed that, when local  
339 coefficients are used, the Perez et al. [4] model showed the lowest RMSE (4.93 %)  
340 followed by the model of Ruiz et al. (Model 1, 4.97 %) [10].

341

342 Table 14. Evaluation of the diffuse luminous efficacy models for all skies

Model	Original coefficients		Local coefficients	
	MBE (%)	RMSE (%)	MBE (%)	RMSE (%)
Perez et al.	1.98	6.42	-0.26	4.93
Ruiz et al. (Model 1)	6.50	15.11	-0.32	4.97

Robledo and Soler (Model 2)	10.81	13.75	-0.48	5.11
Robledo and Soler (Model 1)	9.11	12.02	-0.71	5.12
Ruiz et al. (Model 2)	5.57	8.69	-0.72	5.13
Chaiwiwatworakul and Chirattananon	9.54	13.88	0.03	5.77
Cucumo et al.	8.67	14.61	-1.74	6.67
Fakra et al.	19.39	26.71	-1.74	6.67
Kong and Kim	6.12	15.43	-0.64	6.69
Mayhoub and Carter (Model 1)	4.70	10.60	-0.62	6.90
Muneer and Kinghorn	6.39	11.92	1.03	8.09
Mayhoub and Carter (Model 2)	5.68	11.30	1.17	8.14

343

344 Table 15 shows the results obtained for the case of clear sky (five models). The models  
 345 with the lowest RMSE values, when local coefficients are employed, are those of  
 346 Robledo and Soler [9] (5.35 % and 5.40 %) followed by the Souza and Robledo model  
 347 [11] (5.43 %).

348

349

Table 15. Evaluation of the diffuse luminous efficacy models for clear skies

Model	Original coefficients		Local coefficients	
	MBE (%)	RMSE (%)	MBE (%)	RMSE (%)
Robledo and Soler (Model 1)	31.61	32.30	0.11	5.35
Robledo and Soler (Model 2)	24.56	26.16	0.58	5.40
Souza and Robledo	97.26	100.77	0.57	5.43
Chung	4.82	12.45	-3.13	9.20
Lam and Li	6.93	16.22	-4.10	9.75

350

351 Table 16 shows the results obtained for the case of partly cloudy sky (two models). Using  
 352 the local coefficients, the Robledo and Soler [9] model yielded the lowest RMSE value  
 353 (6.16 %).

354

355

Table 16. Evaluation of the diffuse luminous efficacy models for partly cloudy skies

Model	Original coefficients		Local coefficients	
	MBE (%)	RMSE (%)	MBE (%)	RMSE (%)
Robledo and Soler	7.71	11.47	-0.70	6.16
Chung	4.31	8.88	0.48	6.23

356

357 Table 17 shows the results obtained for the overcast sky conditions (three models).  
 358 Using local coefficients, the Chung [5] and the Robledo and Soler models [9] yielded the  
 359 lowest RMSE values, respectively, 2.64% and 2.85%.

360

361

Table 17. Evaluation of the diffuse luminous efficacy models for overcast skies

Model	Original coefficients		Local coefficients	
	MBE (%)	RMSE (%)	MBE (%)	RMSE (%)
Chung	-6.20	7.69	-0.07	2.64
Robledo and Soler	11.08	12.56	-0.21	2.85
Lam and Li	0.10	4.35	0.14	4.35

362

363 As was expected *a priori*, from the results obtained in Tables 14-17, it can be affirmed  
 364 that the models fitted with data from the local measurements provided lower RMSE  
 365 values than those obtained when using original coefficients.

366

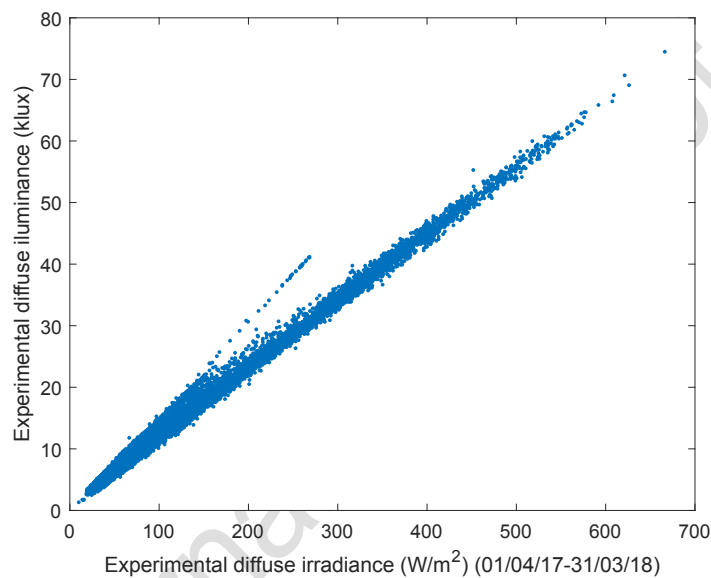
## 367 **6. Proposal of a new model to predict diffuse luminous efficacy**

368 In this section, a new model is proposed to predict diffuse luminous efficacy on horizontal  
 369 surfaces. The dependence of diffuse luminous efficacy ( $K_d$ ) on different variables (solar  
 370 altitude, clearness index, sky clearness, sky brightness, zenith angle, diffuse fraction,  
 371 etc.) was analysed and several models were tested, in order to obtain the final model.  
 372 From these studies, a model for obtaining the luminous efficacy value was proposed.  
 373 This new model is based on a sigmoidal function that employs the solar altitude ( $\alpha$ ) and  
 374 the diffuse fraction ( $D$ ) as the independent variables. In first place, it may be highlighted  
 375 that the proposed model has a determinist term ( $p_0$ ). As can be seen in the present work,  
 376 that term is similar to the value obtained with the models that propose the use of only  
 377 one constant to model luminous efficacy. However, the fact of considering a single  
 378 constant for modelling luminous efficacy means that proper modelling of the behaviour  
 379 of luminous efficacy throughout the day is not possible. In the case of the new model,  
 380 there are another two variables, in addition to a determinist term. One of those variables  
 381 is the diffuse fraction ( $D$ ), as Equation (10) shows, which is defined as the ratio of  
 382 horizontal diffuse irradiance to horizontal global irradiance, and which can be used to  
 383 define the clearness of the sky. The other variable that the model employs is solar altitude  
 384 ( $\alpha$ ). In addition, solar altitude varies throughout the day and, as a result, in some way  
 385 takes the amount of incident surface energy into account. The function that models the  
 386 behaviour of luminous efficacy better than any other can be seen to be a function of a

387 sigmoidal type, for data gathered in Burgos. Its advantage is that two easily obtained  
 388 independent variables are employed, as most radiometric facilities are able to obtain  
 389 both global and diffuse irradiance and the solar altitude can be easily determined.

390 Figure 3 shows the experimental diffuse illuminance versus the experimental diffuse  
 391 irradiance on the horizontal surface at Burgos. As previously mentioned, measurements  
 392 gathered from 1<sup>st</sup> April 2017 to 31<sup>st</sup> March 2018 were employed to develop the models  
 393 and measurements gathered from 1<sup>st</sup> April 2018 to 31<sup>st</sup> December 2018 to test the  
 394 models. The model was firstly proposed for all sky conditions and then applied for  
 395 particular sky conditions (clear, partly cloudy, and overcast).

396



397

398 Figure 3. Experimental diffuse illuminance vs experimental diffuse irradiance on the horizontal surface at  
 399 Burgos

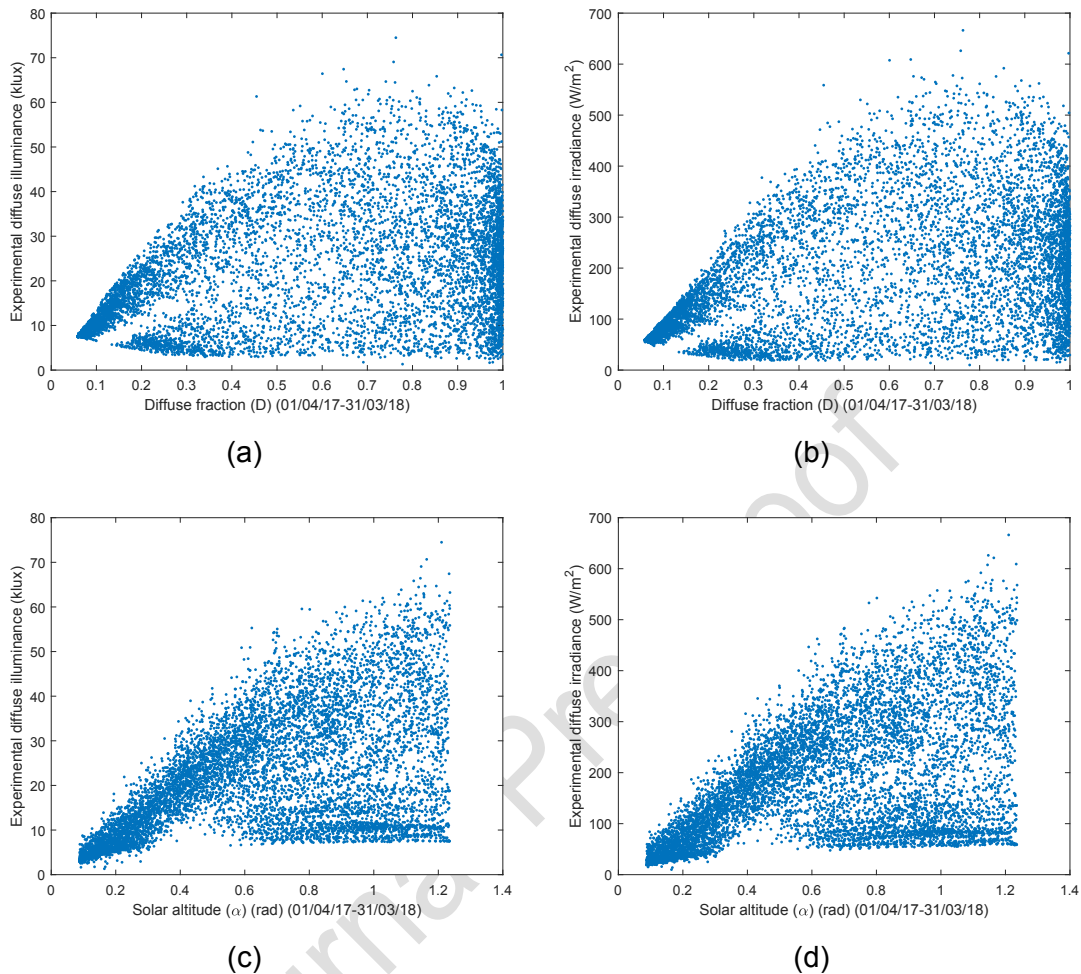
400

401 Figures 4a and 4b depict the experimental diffuse illuminance and irradiance vs. diffuse  
 402 fraction ( $D$ ) at Burgos (Spain) and Figures 4c and 4d depict the experimental diffuse  
 403 illuminance and irradiance vs. solar altitude ( $\alpha$ ) at Burgos (Spain). In figures 4a and 4b,  
 404 it can be seen that the experimental values of illuminance and irradiance present a  
 405 similar behaviour, as would be expected. In addition, the values are lower for clear skies,  
 406 which is logical because the diffuse component was lower. In the case of partly cloudy  
 407 and overcast skies, higher values of both illuminance and irradiance can be seen, with  
 408 greater variability, as a consequence of the sky conditions.

409 With respect to the experimental data of illuminance and irradiance versus solar altitude,  
 410 it may be seen that the lower the values of both illuminance and irradiance, the lower the  
 411 value of solar altitude and with less variability than the values observed when the solar

412 altitude increases, which is logical, as the sky conditions will affect illuminance and  
 413 irradiance to a greater extent.

414



415 Figure 4. (a,b) Experimental diffuse illuminance and irradiance vs. diffuse fraction ( $D$ )  
 416 at Burgos (Spain) and (c,d) Experimental diffuse illuminance and irradiance vs. solar  
 417 altitude ( $\alpha$ ) at Burgos (Spain)

418

### 419 6.1. All sky conditions

420 Equation (10) shows the general form of the new diffuse luminous efficacy model: firstly  
 421 proposed to determine the diffuse illuminance on horizontal surfaces for all sky  
 422 conditions; and, subsequently adjusted for specific sky conditions (clear, partly cloudy,  
 423 and overcast). As will be shown, this model can feasibly be employed for any of the  
 424 above sky conditions. It can be observed that the independent variables of the new  
 425 model are the solar altitude ( $\alpha$ ) and the diffuse fraction ( $D$ ), defined by Equation (6). The  
 426 local model adjusted to the city of Burgos is shown by Equation (11).

427

$$K_d = p_0 + \frac{p_1}{1 + e^{(p_2 \sin(\alpha) + p_3 D)}} \quad (lm/W) \quad (10)$$

428

$$K_d = 112.018 + \frac{271.743}{1 + e^{(2.637 \sin(\alpha) + 4.569 D)}} \quad (lm/W) \quad (11)$$

429

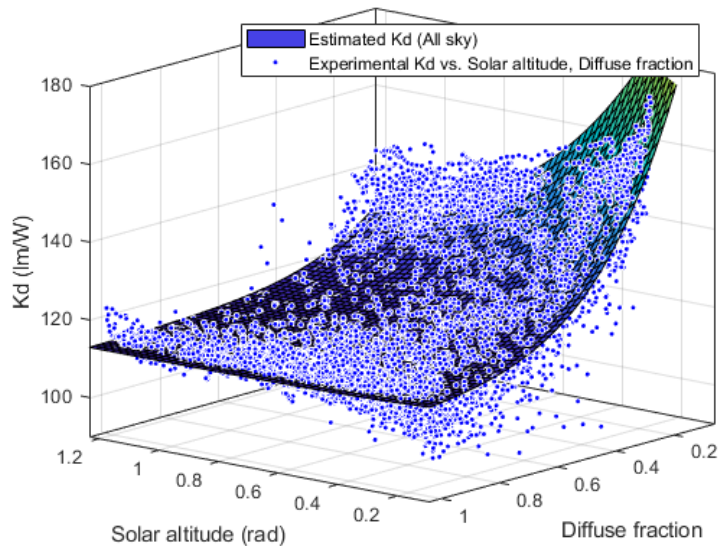
430 With the new model, shown in Equation (11), values of RMSE = 4.77 % and MBE = -  
 431 0.10 % were obtained for all sky types. It can be observed from both Table 14 and  
 432 Table 18 that the RMSE obtained with this new model was lower than any of the all sky  
 433 classic models considered in this present study (twelve models). Figure 5 shows the  
 434 estimated surface and the experimental data. The new model provides good estimations  
 435 of the experimental data.

436

437 Table 18. Comparison between the best performing model for all sky conditions vs the new model for all  
 438 sky conditions

Model	Local coefficients	
	MBE (%)	RMSE (%)
<b>New model, All sky - Equation (11)</b>	<b>-0.10</b>	<b>4.77</b>
Perez et al.	-0.26	4.93

439



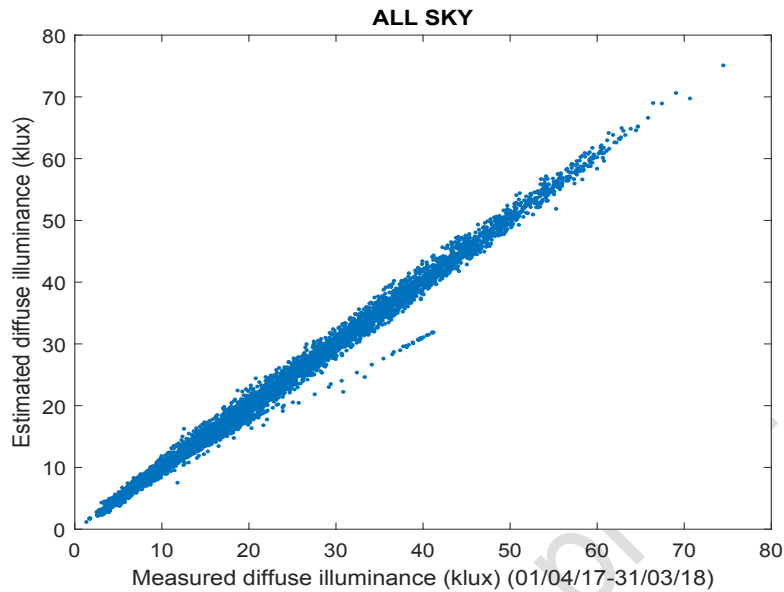
440

441 Figure 5.- Estimated diffuse luminous efficacy using the new model for all sky conditions, Equation (11),  
 442 and experimental values for all sky conditions.

443

444 Figure 6 shows the estimated diffuse illuminance with the new model versus measured  
 445 diffuse illuminance for all sky conditions. As can be observed, the new model adequately  
 446 predicts the diffuse illuminance values for all sky conditions.

447



448

449 Figure 6.- Estimated diffuse illuminance with the new model vs measured diffuse illuminance for all sky  
 450 conditions

451

452 From the results presented above, it can be concluded that the new model proposed in  
 453 Equation (11) yields acceptable predictions of diffuse illuminance for all sky types and  
 454 fitted the experimental data gathered in Burgos, Spain.

455

456 The data were fitted with the non-linear least-squares method using the  
 457 Matlab™ R2018b fit function. For each type of sky, the data were selected with the  
 458 specific sky conditions and had previously been filtered. In each case, it was necessary  
 459 to select the variables that would be used. In the case of our model, the variables were  
 460 defined as solar altitude and diffuse fraction. Those variables are two data vectors that  
 461 will have been filtered by sky type. With the results and the experimental data on  
 462 luminous efficacy ( $K_d$ ), previously obtained and likewise filtered, the adjustment can be  
 463 made by using the Matlab™ R2018b functions.

464

## 465 **6.2. Clear sky**

466 Equation (12) shows the new model, locally adapted for the clear sky condition, defined  
 467 from ( $\varepsilon > 5$ ). This sky condition is employed by the models of Robledo and Soler [9] that  
 468 have the lowest RMSE values of all the models shown in Table 15. The new model,  
 469 which is shown in Equation (12) yields an MBE = 0.14 % and an RMSE = 5.34 %. As

470 can be observed, the RMSE was slightly lower than those obtained with the models of  
 471 Robledo and Soler [9]. Moreover, as can be observed from Table 19, the new model in  
 472 Equation (11), locally fitted for all sky conditions, yields an RMSE value close to those  
 473 locally fitted for a clear sky.

474

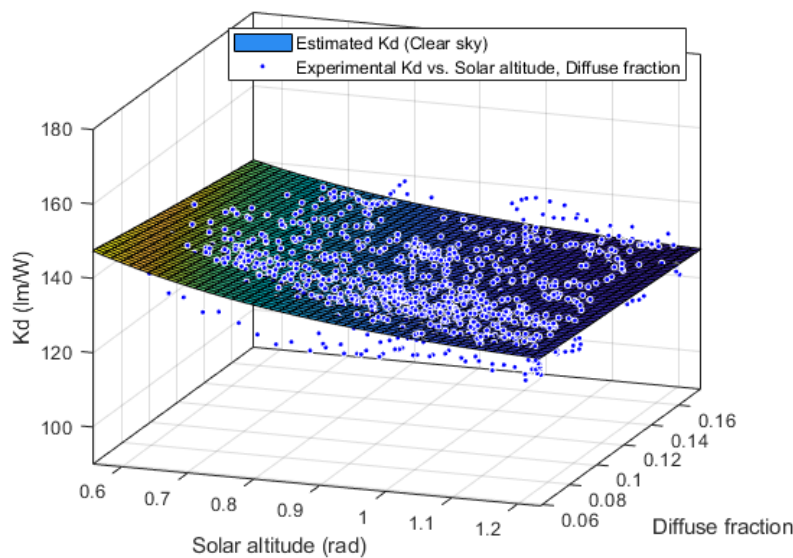
$$K_d = 123.114 + \frac{190.220}{1 + e^{(3.252\sin(\alpha) + 3.340D)}} \quad (lm/W) \quad (12)$$

475

476 Table 19. Comparison between the best performing model for clear sky vs the new model (same sky  
 477 conditions  $\varepsilon > 5$ )

Model	Local coefficients	
	MBE (%)	RMSE (%)
<b>New model, Clear sky - Equation (12)</b>	<b>0.14</b>	<b>5.34</b>
Robledo and Soler (Model 1)	0.11	5.35
New model, All sky - Equation (11)	-1.32	5.92

478



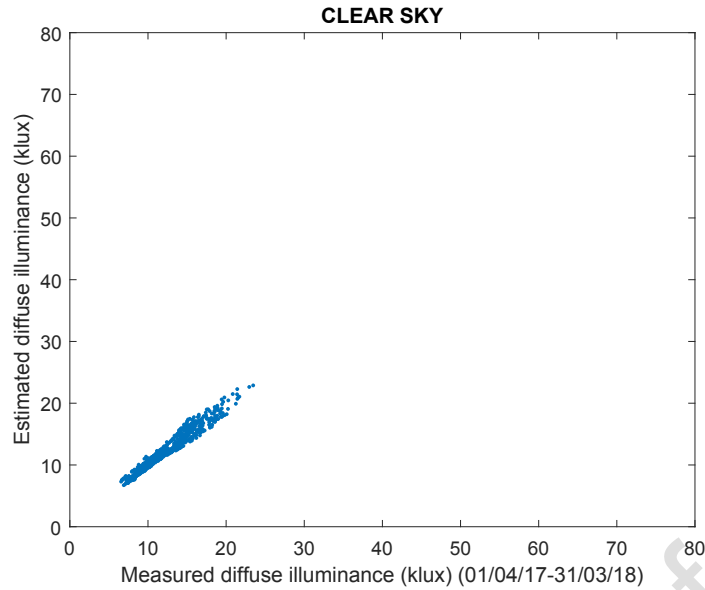
479

480 Figure 7.- Estimated diffuse luminous efficacy using the new model for clear sky, Equation (12), and  
 481 experimental values for clear sky

482

483 Figure 7 shows the estimated luminous efficacy by using the new model, which is shown  
 484 in Equation (12) for clear sky as well as the experimental values. Likewise, Figure 8  
 485 shows the estimated diffuse illuminance with the new model versus the measured diffuse  
 486 illuminance for clear sky conditions.

487



488

489

Figure 8.- Estimated diffuse illuminance using the new model vs measured diffuse illuminance for clear sky conditions given by  $\varepsilon > 5$

490

491

### 492 6.3. Partly cloudy sky

493

494

495

496

497

498

499

500

Equation (13) shows the new model locally fitted for partly cloudy sky conditions, defined by  $(1.2 < \varepsilon < 5.0)$ , which is the sky condition employed by the model of Robledo and Soler [9], because that model has the lowest RMSE values of all the models shown in Table 16. The new model, shown by Equation (13) yields an RMSE value of 5.76 %. Moreover, as shown in Table 20, the new model in Equation (11), locally fitted for all sky conditions, yields an RMSE value of 5.98 %; both slightly lower than the values obtained with the model of Robledo and Soler [9].

$$K_d = 108.635 + \frac{240.293}{1 + e^{(2.515 \sin(\alpha) + 3.656D)}} \quad (lm/W) \quad (13)$$

501

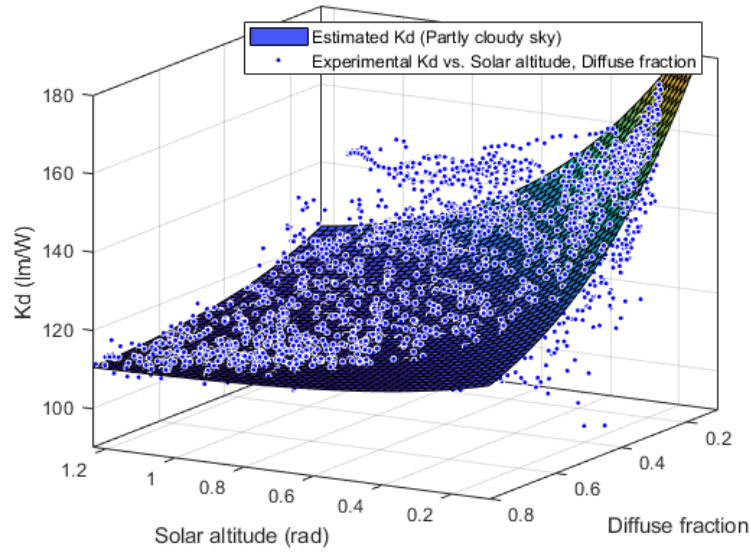
502

503

Table 20. Comparison between the best performing model for partly cloudy sky and the new model, using the same sky conditions  $(1.2 < \varepsilon < 5.0)$

Model	Local coefficients	
	MBE (%)	RMSE (%)
<b>New model, Partly cloudy sky - Equation (13)</b>	<b>-0.38</b>	<b>5.76</b>
New model, All sky - Equation (11)	-0.74	5.98
Robledo and Soler	-0.70	6.16

504



505

506

Figure 9.- Estimated diffuse luminous efficacy using the new model for partly cloudy sky, Equation (13), and experimental values for partly cloudy sky

507

508

509 Figure 9 shows the estimated luminous efficacy using the new model, which is shown in

510 Equation (13) for partly cloudy sky, as well as the experimental values. Likewise,

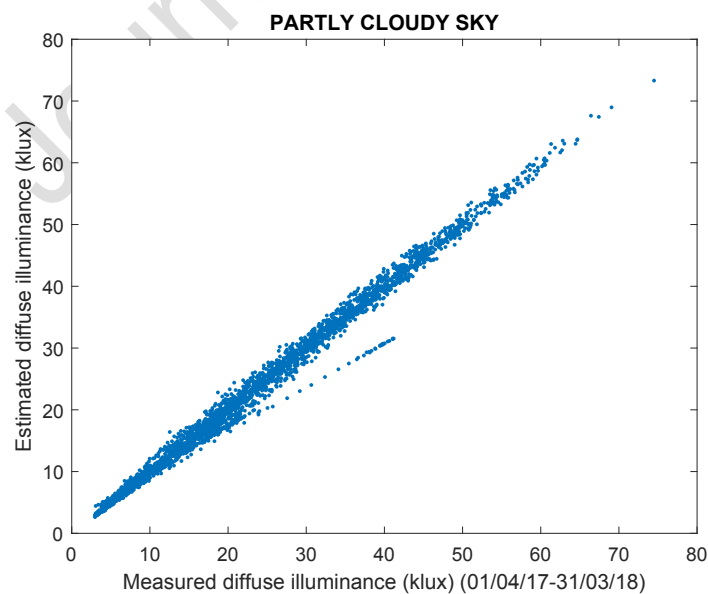
511 Figure 10 shows the estimated diffuse illuminance with the new model versus measured

512 diffuse illuminance for partly cloudy sky conditions. It can be observed that the new

513 model, given by Equation (13), produces acceptable predictions of the diffuse

514 illuminance values for partly cloudy skies.

515



516

517

Figure 10.- Estimated diffuse illuminance with the new model vs measured diffuse illuminance for partly cloudy sky conditions ( $1.2 < \varepsilon < 5.0$ )

518

519

520

521 **6.4. Overcast sky conditions**

522 Equation (14) shows the new model locally fitted for overcast sky conditions given by ( $D$   
 523  $> 0.8$ ), which are those employed by the Chung Model [5], because this model yielded  
 524 the lowest RMSE (2.64 %) from among those shown in Table 17. The new model in  
 525 Equation (14) yields an RMSE value of 2.83 %, slightly higher than the previous one.  
 526 Moreover, as can be observed in Table 21, an RMSE of 2.96 % was attained with the  
 527 new model locally fitted with all data (all sky conditions). It can therefore be noted that  
 528 these RMSE values are similar to those obtained by the Chung Model [5].

529

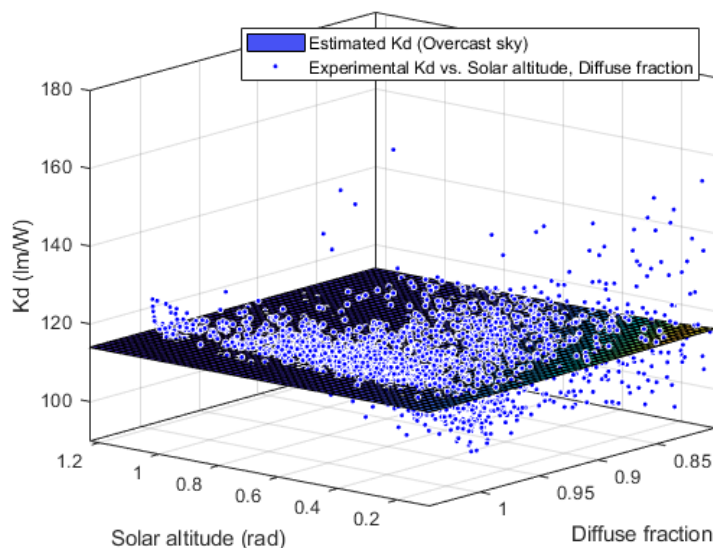
$$K_d = 113.516 + \frac{203.807}{1 + e^{(3.296\sin(\alpha) + 5.712D)}} \quad (lm/W) \quad (14)$$

530

531 Table 21. Comparison between the best performing model for overcast skies and the new model, using the  
 532 same sky conditions ( $D > 0.8$ )

Model	Local coefficients	
	MBE (%)	RMSE (%)
Chung Model	-0.07	2.64
<b>New model, Overcast sky - Equation (14)</b>	<b>-0.06</b>	<b>2.83</b>
New model, All sky - Equation (11)	-0.73	2.96

533

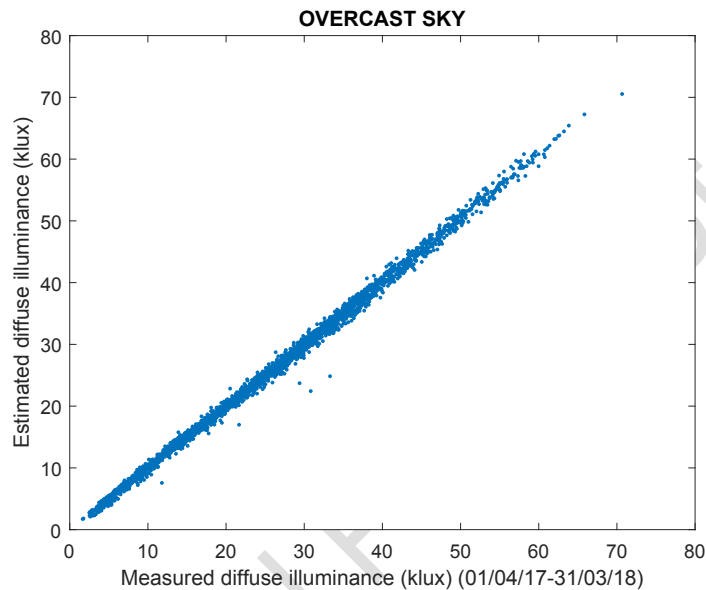


534

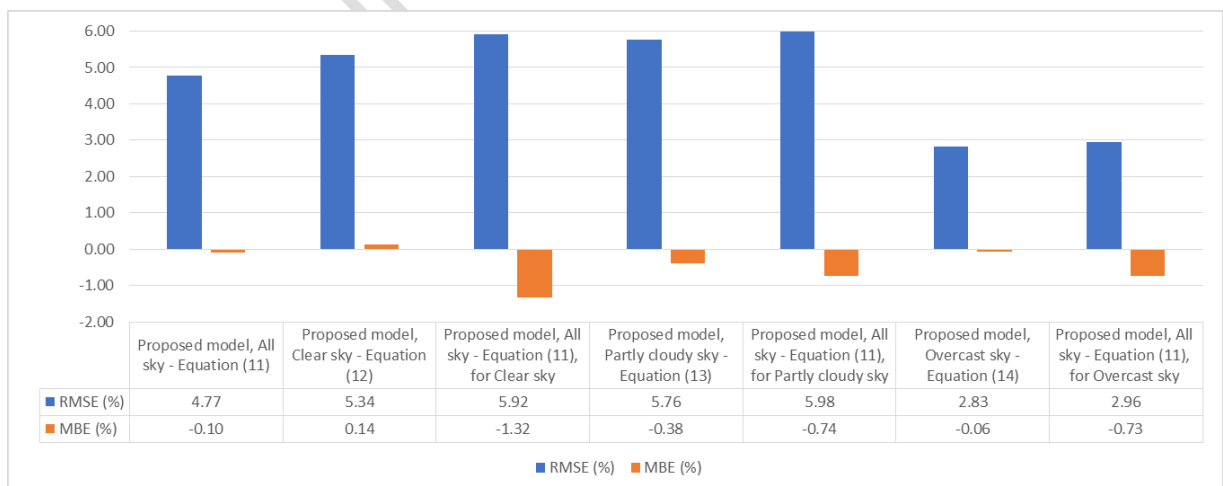
535 Figure 11.- Estimated diffuse luminous efficacy using the new model for overcast sky, Equation (14), and  
 536 experimental values for overcast sky

537

538 Figure 11 shows the estimated luminous efficacy using the new model, which is shown  
 539 in Equation (14) for overcast sky as well as the experimental values. As can be observed,  
 540 this model yields acceptable predictions of luminous efficacy, which is approximately  
 541 constant in the interval defined by the sky ratio. Figure 12 shows the estimated diffuse  
 542 illuminance with the new model versus measured diffuse illuminance for overcast sky  
 543 conditions. As can be noted, the new model is able to predict the diffuse illuminance for  
 544 overcast sky conditions.  
 545



546  
 547 Figure 12.- Estimated diffuse illuminance with the new model vs measured diffuse illuminance for overcast  
 548 sky conditions ( $D > 0.8$ )  
 549



550  
 551 Figure 13.- RMSE (%) and MBE (%) using the new model for the sky conditions analysed in this study  
 552

553 Figure 13 shows a comparison between the RMSE and MBE values using the new model  
 554 for all sky and for particular sky conditions (clear, partly cloudy, and overcast). It can be

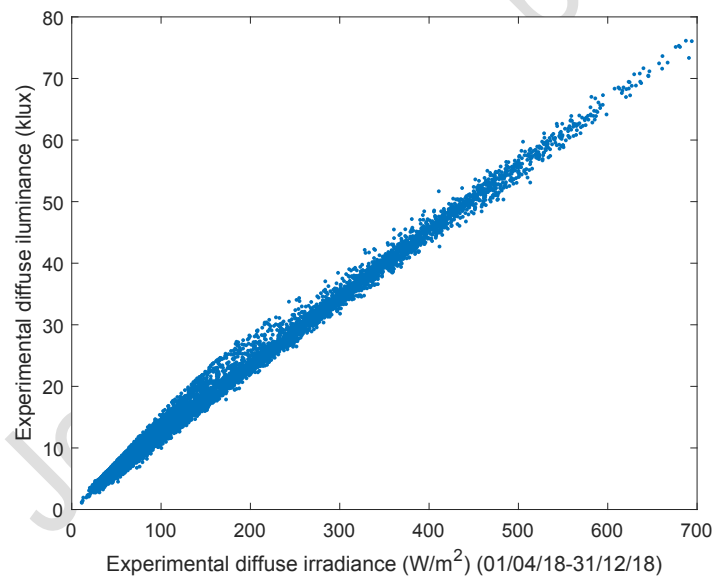
555 observed that the new model provides acceptable predictions of diffuse illuminance both  
 556 for all sky and for particular sky conditions (clear, partly cloudy, and overcast).

557

## 558 **7. Validation of the diffuse illuminance models**

559 In Section 4, the diffuse luminous efficacy models from twenty-two existing models in the  
 560 literature were fitted to local data from Burgos (Spain) and, in Section 5, the same models  
 561 were evaluated. In Section 6, a new model was fitted and analysed for all sky and for  
 562 particular sky conditions, using the same data as the previously mentioned models. In  
 563 this Section, all of these models will now be validated by employing nine months of  
 564 additional measurements gathered between 1<sup>st</sup> April 2018 and 31<sup>st</sup> December 2018.  
 565 These measurements were taken, following the same procedure described in Section 3.  
 566 Figure 14 shows the experimental data employed for testing the global luminous efficacy  
 567 models. The figure shows measured diffuse illuminance versus measured diffuse  
 568 irradiance on the horizontal surface at Burgos over the test period.

569



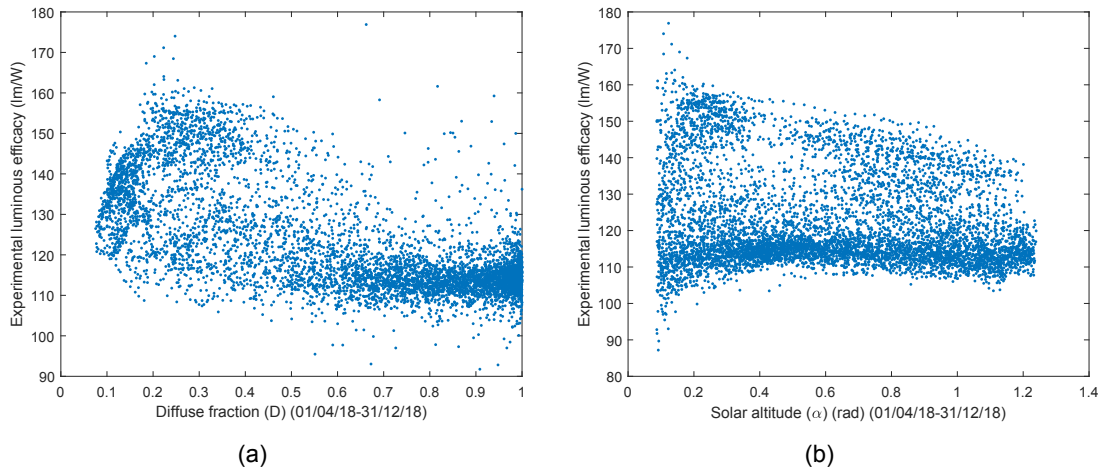
570

571 Figure 14.- Experimental diffuse illuminance vs experimental diffuse irradiance on the horizontal surface at  
 572 Burgos (test period)

573

574 As can be observed, Figure 15(a) shows the experimental diffuse luminous efficacy  
 575 versus the diffuse fraction and Figure 15(b) shows the experimental diffuse luminous  
 576 efficacy versus solar altitude, both for all sky conditions, using data gathered during the  
 577 test period.

578



579 Figure 15.- (a) Experimental diffuse luminous efficacy vs Diffuse fraction (D) and (b) Experimental diffuse  
 580 luminous efficacy vs solar altitude ( $\alpha$ ) for all sky (test period)

581

582 Data from these additional nine months of measurement are used to re-evaluate both  
 583 RMSE and MBE in the models previously fitted with experimental data (local models), in  
 584 order to validate the results. Tables 22-25 present the results of evaluating the statistical  
 585 estimators shown in Equation (8) and in Equation (9) using the luminous efficacy models  
 586 analysed in this study. The results obtained from the different sky conditions under study  
 587 are also shown. To that end, the specific sky conditions proposed by each author were  
 588 applied, in order to define the different sky types (clear sky, partly cloudy sky, and  
 589 overcast sky). The new model proposed in this study was also validated both for all sky  
 590 conditions and for particular sky types (clear, partly cloudy, and overcast). In the latter  
 591 case, the conditions employed by the model with the lowest RMSE value were used to  
 592 define the sky type. Table 22 shows the MBE and RMSE results of the tests for all sky  
 593 conditions using the twelve classic models and the new model. It is shown in the  
 594 validation that, the model of Perez et al. [4] (4.32 %) provided slightly lower results than  
 595 the new model (4.44 %).

596

597

Table 22. Validation of the diffuse luminous efficacy models for all skies

Model	Local coefficients	
	MBE (%)	RMSE (%)
Perez et al.	-0.51	4.32
New model, All sky – Equation (11)	-0.90	4.44
Ruiz et al. (Model 1)	-1.28	4.97
Robledo and Soler (Model 2)	-1.55	5.04
Robledo and Soler (Model 1)	-1.86	5.21
Ruiz et al. (Model 2)	-1.87	5.22

Chaiwiwatworakul and Chirarattananon	-1.06	5.39
Cucumo et al.	-1.90	6.74
Fakra et al.	-1.90	6.74
Mayhoub and Carter (Model 1)	-0.78	6.93
Kong and Kim	-2.36	7.33
Muneer and Kinghorn	0.29	8.11
Mayhoub and Carter (Model 2)	0.49	8.14

598

599 The results obtained from classic clear sky models (five models) and the new model are  
600 shown in Table 23. In addition, the results from the validation of the all sky model, given  
601 by Equation (11) for this particular sky type are also compared. It is shown that the  
602 models with the lowest RMSE values were those of the Souza and Robledo model [11]  
603 (5.89 %) and the Robledo and Soler model (Model 2) [9] (5.89 %). The new model given  
604 by Equation (12) yielded similar values to those obtained with the previously mentioned  
605 models (5.97 %). Moreover, the model obtained for all sky conditions provided an RMSE  
606 value of (6.90 %), higher than the one obtained with particular sky conditions given by ( $\varepsilon$   
607  $> 5$ ), which were used by Souza and Robledo [11] and Robledo and Soler [9].

608

609

Table 23. Validation of the diffuse luminous efficacy models for clear sky conditions

Model	Local coefficients	
	MBE (%)	RMSE (%)
Souza and Robledo	0.32	5.89
Robledo and Soler (Model 2)	0.27	5.89
Robledo and Soler (Model 1)	-0.54	5.96
New model, Clear sky – Equation (12)	-0.52	5.97
New model, All sky – Equation (11)	-2.66	6.90
Chung	-4.64	9.59
Lam and Li	-4.62	9.79

610

611 Likewise, Table 24 shows the results obtained for classic partly cloudy sky models. It can  
612 be noted that the model with the lowest RMSE value is the new model for all sky  
613 conditions, defined by Equation (11) (5.72 %), followed by the new model for partly  
614 cloudy sky, defined by Equation (13) (6.01 %) and the Chung model [5] (6.01 %).

615

616

Table 24. Validation of the diffuse luminous efficacy models for partly cloudy sky

Model	Local coefficients	
	MBE (%)	RMSE (%)

New model, All sky – Equation (11)	-1.00	5.72
New model, Partly cloudy sky - Equation (13)	1.88	6.01
Chung	-1.21	6.01
Robledo and Soler	-2.51	6.35

617

618

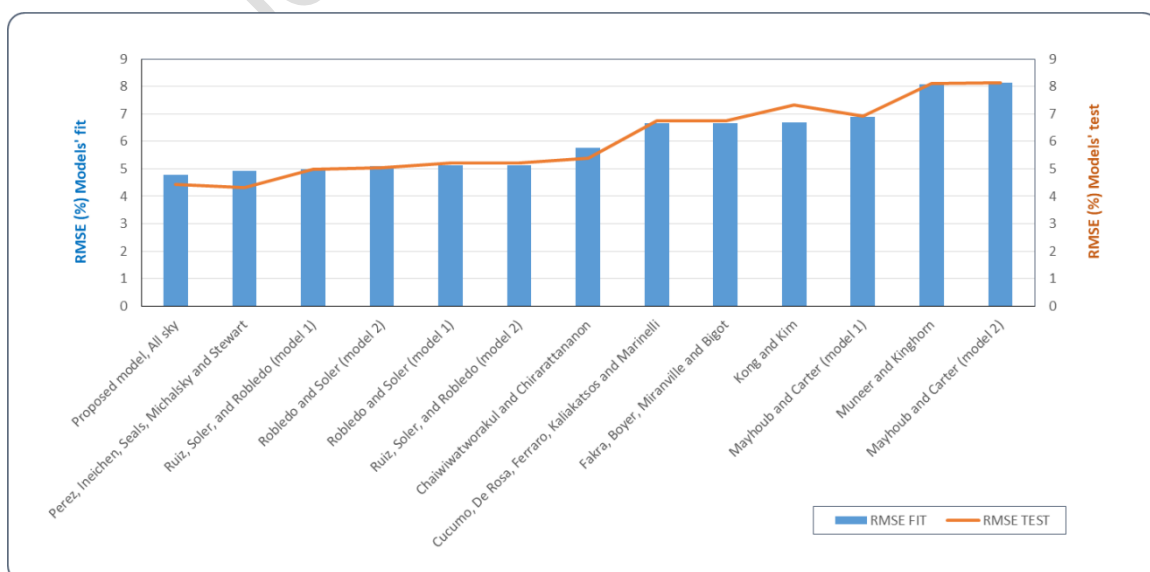
Table 25. Validation of the diffuse luminous efficacy models for overcast sky

Model	Local coefficients	
	MBE (%)	RMSE (%)
Chung	-0.25	2.44
Robledo and Soler	-0.43	2.78
New model, All sky – Equation (11)	-0.80	2.93
New model, Overcast sky - Equation (14)	1.06	3.19
Lam and Li	-0.02	3.79

619

620 Finally, Table 25 shows the results obtained for the classic overcast sky models (three  
621 models), which are also compared with the new models. It can be noted that the model  
622 with the lowest RMSE values is the model of Chung [5] (2.44 %). Moreover, it can be  
623 observed that the models proposed in this present study fitted both for all sky conditions  
624 (2.93 %) and for overcast sky conditions (3.19 %) provide similar values to those of the  
625 Chung model [5]. As Figure 16 shows, in the case of all sky conditions, both the classic  
626 models and the new models analysed in this study with data from the test period present  
627 a similar tendency to that observed with data gathered to fit the models. A similar  
628 behaviour was also attained for particular sky conditions (clear, partly cloudy, and  
629 overcast).

630



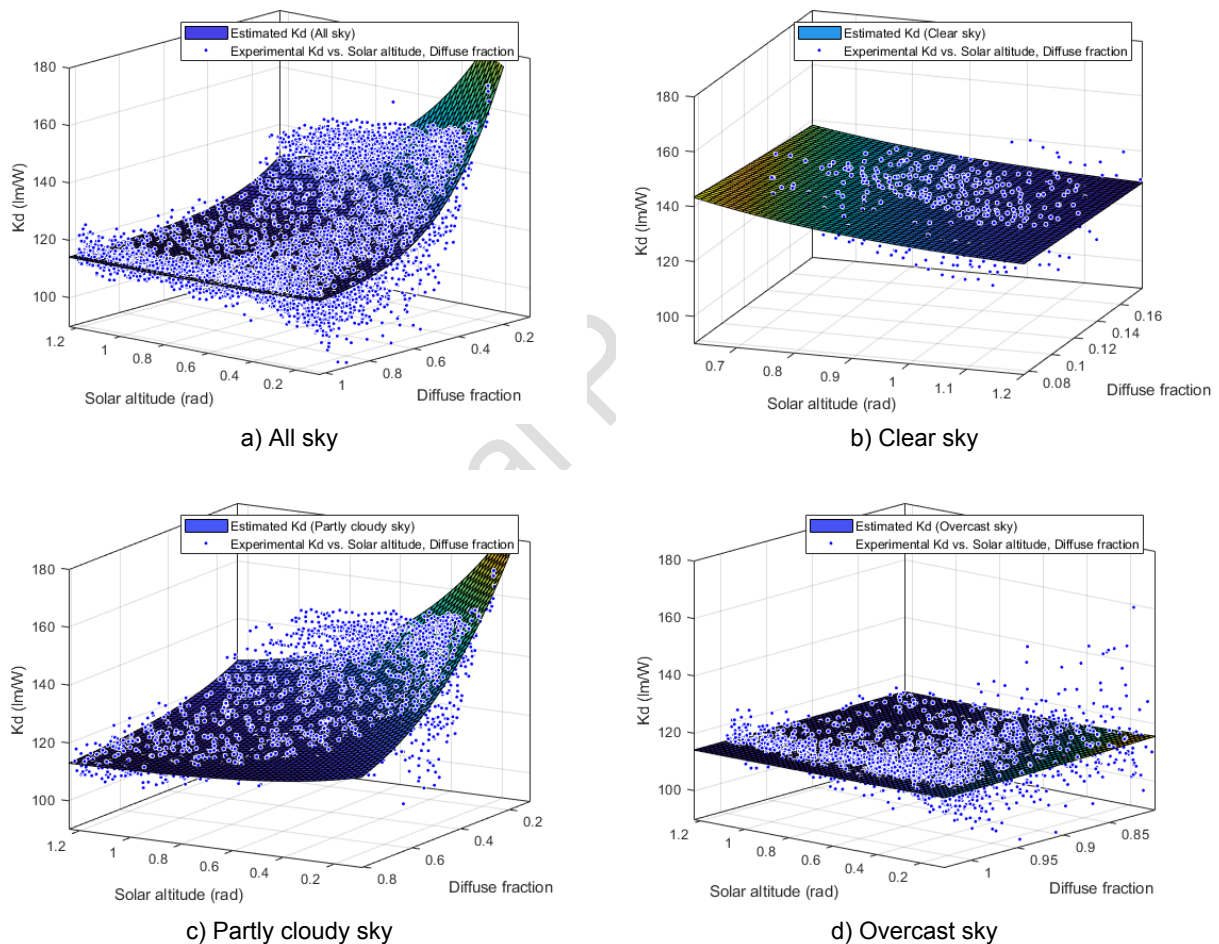
631

632 Figure 16.- Comparison between the RMSE values obtained with the classic models and the new model in  
 633 the fit period (1<sup>st</sup> April 2017 to 31<sup>st</sup> March 2018) and in the validation period (1<sup>st</sup> April 2018 to 31<sup>st</sup>  
 634 December 2018)

635

636 Figure 17 shows the results obtained with the data gathered during the test period (1<sup>st</sup>  
 637 April 2018 - 31<sup>st</sup> December 2018). These figures were obtained both for all sky and for  
 638 particular sky conditions using the new models developed in this present study. These  
 639 figures show the experimental measurements and the estimated diffuse luminous  
 640 efficacy. A similar behaviour to the one obtained with the data employed to fit the models  
 641 (1<sup>st</sup> April 2017 to 31<sup>st</sup> March 2018) can be observed.

642



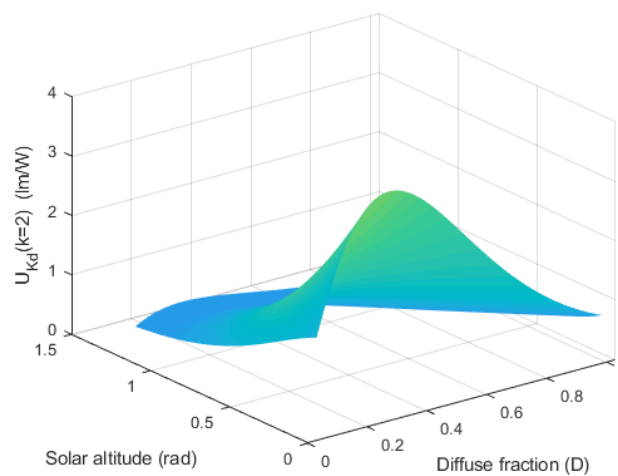
643

644 Figure 17.- Estimated  $K_d$  and measured values for all sky and for particular sky conditions using  
 645 measurements gathered in the test period (1<sup>st</sup> April 2018 - 31<sup>st</sup> December 2018).

646

647 In addition, state of the art literature was consulted and the uncertainty values for solar  
 648 altitude proposed in the work of H. Kambezidis, 2012 [24], were selected. Likewise, the  
 649 results that are shown in both the pyranometer manual [25] and the state of the art: I.

650 Reda [26] and T. Muneer et al. [27] were considered, to account for the uncertainty of  
 651 the irradiance measurement in the experimental measurements. On the basis of those  
 652 uncertainty values, the uncertainty of the diffuse fraction ( $D$ ) may be calculated. This  
 653 uncertainty, together with the uncertainty of the solar altitude, makes it possible to  
 654 evaluate the uncertainty of the luminous efficacy model proposed in this work. Having  
 655 determined the uncertainty, a graphic representation of the values that our model yields  
 656 is possible. Therefore, when evaluating the data collected over the test period (01/04/18-  
 657 31/12/18), the uncertainty of the model adopts a form that is shown in Figure 18. The  
 658 uncertainty values that the model provides are relatively small in relation to the values of  
 659 luminous efficacy. It may therefore be affirmed that the proposed model is acceptable.



660  
 661 Figure 18. Luminous efficacy uncertainty of the proposed model for all sky conditions  
 662

## 663 8. Conclusions

664 In this present study, twenty-two classic diffuse luminous efficacy models from the  
 665 existing literature have been evaluated, both with their original coefficients and locally  
 666 adapted coefficients estimated from the experimental data recorded at Burgos (Spain),  
 667 between 1<sup>st</sup> April 2017 and 31<sup>st</sup> March 2018. The local behaviour of the models has been  
 668 noted, which leads to lower RMSE and MBE values than those obtained by using their  
 669 original coefficients.

670

671 A new diffuse luminous efficacy model has been proposed and analysed in this present  
 672 study, in order to predict the illuminance on horizontal surfaces. This new model has  
 673 been fitted for all sky types and for particular sky types (clear, partly cloudy, and  
 674 overcast). This new model employs two independent variables: the diffuse fraction ( $D$ ),  
 675 which is easily obtained from most radiometric facilities that can measure both global

676 and diffuse irradiance, and the solar altitude ( $\alpha$ ) that is also easily obtained whatever the  
677 geographical location.

678

679 The new model fitted with data collected during the period (1<sup>st</sup> April 2017 - 31<sup>st</sup> March  
680 2018) yields an RMSE value lower than any of the classic models analysed in this study  
681 for all sky conditions, as can be observed in Table 18. Moreover, the new model initially  
682 proposed for all sky conditions, shown in Equation (11), could be used either for all sky  
683 or for particular sky conditions (clear, partly cloudy, and overcast).

684

685 In turn, the new model fitted for particular sky conditions (clear, partly cloudy and  
686 overcast), with the data collected during the period (1<sup>st</sup> April 2017 - 31<sup>st</sup> March 2018),  
687 provides lower RMSE results than any of the classic models analysed in this study for  
688 clear sky and partly cloudy sky and it yields similar values in the case of overcast sky  
689 than the best performing models for this particular sky condition.

690

691 The models yielded similar RMSE values both for the results of the validation data  
692 recorded during the period between 1<sup>st</sup> April 2018 and 31<sup>st</sup> December 2018 and for the  
693 data recorded between 1<sup>st</sup> April 2017 and 31<sup>st</sup> March 2018, for all sky conditions, as  
694 shown in Figure 16. Likewise, a similar behaviour was observed for particular sky  
695 conditions (clear sky, partly cloudy and overcast sky).

696

## 697 **Acknowledgements**

698 The authors acknowledge the financial support from the Spanish Government (Ministerio  
699 de Economía y Competitividad) (ENE2014-54601-R). David González Peña would also  
700 like to thank the Junta de Castilla-León for economic support (PIRTU Program, ORDEN  
701 EDU/310/2015)

702

## 703 **References**

- 704 1. He, Y., A. Wang, and H. Huang, *The trend of natural illuminance levels in 14 Chinese cities*  
705 *in the past 50 years*. Energy, Sustainability and Society, 2013. **3**(1): p. 1-11.
- 706 2. Fabian, M., Y. Uetani, and S. Darula, *Monthly luminous efficacy models and illuminance*  
707 *prediction using ground measured and satellite data*. Solar Energy, 2018. **162**: p. 95-108.
- 708 3. Ward, G.J. and R.A. Shakespeare, *Rendering With Radiance: The Art And Science Of*  
709 *Lighting Visualization*. 1998: Morgan Kaufman.
- 710 4. Perez, R., et al., *Modeling daylight availability and irradiance components from direct*  
711 *and global irradiance*. Solar Energy, 1990. **44**(5): p. 271-289.

- 712 5. Chung, T.M., *A study of luminous efficacy of daylight in Hong Kong*. Energy and Buildings,  
713 1992. **19**(1): p. 45-50.
- 714 6. Lam, J.C. and D.H.W. Li, *Luminous efficacy of daylight under different sky conditions*.  
715 Energy Conversion and Management, 1996. **37**(12): p. 1703-1711.
- 716 7. Iqbal, M., *Introduction to solar radiation*. 1983: Academic Press.
- 717 8. Muneer, T. and D. Kinghorn, *Luminous efficacy models - Evaluation against UK data*.  
718 Journal of the Illuminating Engineering Society, 1998. **27**(1): p. 163-169.
- 719 9. Robledo, L. and A. Soler, *On the luminous efficacy of diffuse solar radiation*. Energy  
720 Conversion and Management, 2001. **42**(10): p. 1181-1190.
- 721 10. Ruiz, E., A. Soler, and L. Robledo, *Assessment of Muneer's luminous efficacy models in  
722 Madrid and a proposal for new models based on his approach*. Journal of Solar Energy  
723 Engineering, Transactions of the ASME, 2001. **123**(3): p. 220-224.
- 724 11. Souza, R. and L. Robledo, *Testing diffuse luminous efficacy models for Florianópolis,  
725 Brazil*. Building and Environment, 2004. **39**(3): p. 317-325.
- 726 12. De Rosa, A., et al., *Simplified correlations of global, direct and diffuse luminous efficacy  
727 on horizontal and vertical surfaces*. Energy and Buildings, 2008. **40**(11): p. 1991-2001.
- 728 13. Cucumo, M., et al., *Correlations of global and diffuse solar luminous efficacy for all sky  
729 conditions and comparisons with experimental data of five localities*. Renewable Energy,  
730 2008. **33**(9): p. 2036-2047.
- 731 14. Fakra, A.H., et al., *A simple evaluation of global and diffuse luminous efficacy for all sky  
732 conditions in tropical and humid climate*. Renewable Energy, 2011. **36**(1): p. 298-306.
- 733 15. Azad, A.S., D. Rakshit, and K.N. Patil, *Model development and evaluation of global and  
734 diffuse luminous efficacy for humid sub-tropical region*. Renewable Energy, 2018. **119**:  
735 p. 375-387.
- 736 16. Mayhoub, M.S. and D.J. Carter, *Methods to estimate global and diffused luminous  
737 efficacies based on satellite data*. Solar Energy, 2011. **85**(11): p. 2940-2952.
- 738 17. Kong, H.J. and J.T. Kim, *Modeling luminous efficacy of daylight for Yongin, South Korea*.  
739 Energy and Buildings, 2013. **62**: p. 550-558.
- 740 18. Patil, K.N., S.N. Garg, and S.C. Kaushik, *Luminous efficacy model validation and  
741 computation of solar illuminance for different climates of India*. Journal of Renewable  
742 and Sustainable Energy, 2013. **5**(6).
- 743 19. Littlefair, P.J., *Measurements of the luminous efficacy of daylight*. Lighting research &  
744 technology, 1988. **20**(4): p. 177-188.
- 745 20. Chaiwiwatworakul, P. and S. Chirarattananon, *Luminous efficacies of global and diffuse  
746 horizontal irradiances in a tropical region*. Renewable Energy, 2013. **53**: p. 148-158.
- 747 21. Dieste-Velasco, M.I., et al., *Performance of global luminous efficacy models and proposal  
748 of a new model for daylighting in Burgos, Spain*. Renewable Energy, 2019. **133**: p. 1000-  
749 1010.
- 750 22. *CIE 108-1994. Technical Report: Guide to recommended practice of daylight  
751 measurement*. Commission Internationale de l'Éclairage. 1994.
- 752 23. López, G. and C.A. Gueymard, *Clear-sky solar luminous efficacy determination using  
753 artificial neural networks*. Solar Energy, 2007. **81**(7): p. 929-939.
- 754 24. Kambezidis, H. *The Solar Resource*. Earth and Planetary Sciences, 2012, 3, p. 27-84. DOI:  
755 10.1016/B978-0-08-087872-0.00302-4.
- 756 25. Huksefluz, *User Manual SR11*, First class pyranometer.
- 757 26. Reda, I., *Method to Calculate Uncertainties in Measuring Shortwave Solar Irradiance  
758 Using Thermopile and Semiconductor Solar Radiometers*, 2011, NREL/TP-3B10-52194,  
759 Technical Report.

- 760 27. Muneer, T., Gueymard, C., Kambezidis, H., *Solar Radiation and Daylight Models (Second*  
761 *Edition)*, 2004, Butterworth-Heinemann.  
762

Journal Pre-proof

## Highlights

- A new model of diffuse luminous efficacy over a horizontal surface is proposed
- A comparative study of twenty-two classic luminous efficacy models is presented
- The proposed model behaves in a better way than most of the classic models analysed
- Diffuse illuminance in all sky and in particular sky conditions can be determined

Journal Pre-proof